RSC Sustainability

ROYAL SOCIETY OF CHEMISTRY

PAPER

View Article Online
View Journal | View Issue

Cite this: *RSC Sustainability*, 2023, **1**, 1773

Sustainable approach for the synthesis of chiral β-aminoketones using an encapsulated chiral Zn(II)–salen complex†

Pratikkumar Lakhani, [a] Sanjeev Kane,[b] Himanshu Srivastava,[b] U. K. Goutam[c] and Chetan K. Modi *[a]

To enable sustainable chemical transformations, it is imperative to adopt ecofriendly strategies aligned with economic growth and environmental preservation. We present a more environmentally conscious method for synthesizing Zn(II)–salen ligand encapsulated within an MWW host as a heterogeneous chiral catalyst, denoted as Zn(II)–salen@MWW. Various techniques, including FTIR, FESEM, EDX, XRD, BET, and XPS were used to confirm the successful chiral Zn(II) ligand encapsulation. Utilizing an uncomplicated ultrasonic approach, the synthesized catalyst efficiently produces chiral β-amino carbonyl compounds at room temperature under solvent-free conditions. The catalytic process takes 120 minutes, yielding an impressive 94% with selectivity >94%. This protocol offers multiple benefits, including an environmentally friendly catalyst, simple setup, easy separation, and the capability to reuse the chiral Zn(II)–salen@MWW catalyst for up to five runs. Substrate tests involving aldehydes, ketones, and anilines exhibit yields ranging from 96% to 80% and selectivity from 96% to 83%. The process holds significant potential for academia and industry.

Received 27th June 2023
Accepted 24th August 2023

DOI: 10.1039/d3su00210a

rsc.li/rscsus

Sustainability spotlight statement

The pursuit of sustainable chemical transformations necessitates the integration of eco-friendly approaches, economic growth, and environmental conservation. In line with this objective, a remarkable breakthrough has been made in the development of a greener decorum for synthesizing the present catalyst. The present heterogeneous chiral catalyst exhibits immense potential for promoting sustainable practices in the field of asymmetric synthesis. The utilization of an unpretentious ultrasonic approach allows the synthesized catalyst to efficiently generate chiral β-amino carbonyl compounds under solvent-free conditions at room temperature. This significantly contributes to the reduction of both energy consumption and the generation of toxic byproducts. Another noteworthy feature is the effortless separation of the catalyst from the reaction mixture, facilitating its recovery and reusability. The ability to reprocess the catalyst for up to five runs not only minimizes waste generation but also optimizes resource utilization. This further reinforces the sustainability aspect of the process, as it promotes the efficient use of materials and reduces the demand for fresh catalyst production. As efforts towards sustainability continue to gain momentum, this innovative approach is poised to play a crucial role in advancing both academic research and industrial practices.

Introduction

Asymmetric catalysis has become highly advanced in recent years, but there are still challenges to overcome in this area, such as developing environmentally safe methods and using substrates that have been considered unreactive.[1] Ketones, in particular, pose a significant challenge to the current state of asymmetric methodologies.[2] Due to their low reactivity and difficulties in restraining facial stereoselectivity, some enantioselective chiral catalytic C–C bond formation reactions with carbonyl are available, despite being effective procedures for enantioselective reduction of ketones.[3] In contrast, salen–metal complexes may be useful as bifunctional Lewis acid–base catalysts for contemporary catalytic reactions with imperative substrates.[4]

Scientists have embraced Green Chemistry principles over the past few decades, and environmental considerations have become part of chemical processes.[5] A significant part of the active pharmaceutical ingredient (API) manufacturing processes relies on the reaction media, which accounts for up to 80% of the total mass.[6,7] To overcome this issue, the major pharmaceutical companies have developed solvent selection guides for drug synthesis chemical processes. The development of clean technologies that replace hazardous organic solvents with environmentally friendly solvents has become increasingly

[a]*Applied Chemistry Department, Faculty of Technology and Engineering, The Maharaja Sayajirao University of Baroda, Vadodara-390001, India. E-mail: chetanmodi-appchem@msubaroda.ac.in*

[b]*Synchrotrons Utilisation Section, Raja Ramanna Centre for Advanced Technology, Indore 452013, India*

[c]*Technical Physics Division, Bhabha Atomic Research Centre, Mumbai-400085, India*

† Electronic supplementary information (ESI) available. See DOI: https://doi.org/10.1039/d3su00210a

popular in recent years.[8] Owing to this new challenge, organic synthesis has become increasingly popular under solvent-free conditions, as "green chemistry" strives to minimize pollution, costs, and tedious procedures.[9,10]

In synthetic organic chemistry, multicomponent reactions (MCRs) are becoming increasingly popular for their many advantages, including increased atom economy, simplicity, structural disparity, energy savings, and waste reduction.[11] MCRs are particularly valuable for the production of distinctly functionalized organic compounds that can succor as valuable heterocyclic forerunners in pharmacology.[12] The Mannich reaction is one such MCR that is widely used for the manufacturing of new-fangled nitrogen-encompassing organic moieties with biological activity.[13] Aminocarbonyl molecules synthesized through the Mannich reaction can be used as intermediates for the synthesis of many important biomolecules, including amino alcohols, amino acids, peptides, and lactams.[14–19] Among the various Mannich reaction catalysts explored, ultrasonic-assisted organic synthesis (UAOS) is an eco-friendly and competent tactic that significantly enhances reaction rates, yields, and selectivity. In recent years, UAOS have been utilized to uphold multi-component self-Mannich reactions and asymmetric Mannich reactions effectively and expeditiously.[20–22]

Considering their improved recyclability, novel heterogeneous catalytic systems such as nanoparticle-supported/encapsulated solid acids, metal nanoparticles, and metal-coordinated polymers have received increasing attention in recent years.[23,24] However, the synthesis of these catalysts limits their practical applications among insoluble bulk materials.[25–27] As a way to solve this problem, micro- and/or meso-porous siliceous substances likes MCM-41, MCM-48, MCM-50, SBA-15, KIT-6, USY zeolite, or MWW-zeolite have been extensively studied because of their unvarying interior pore structure, elevated surface areas, wide-ranging ordered pores with confined size distributions, and superior hydrothermal stability, making them ideal for heterogeneous catalysts. This study uses zinc metal ions as Lewis acids, which are highly potent, low-cost, non-toxic, and soft enough and therefore, suited for Mannich reaction. Herein, we report a green decorum for synthesizing distinctive Zn(II)–salen ligand encapsulated in MWW host as a heterogeneous chiral catalyst, *i.e.*, Zn(II)–salen@MWW, and employed for the efficient and rapid synthesis of β-amino ketones under measly conditions using an ultrasound-assisted one-pot tactic in solvent-free conditions (Scheme 1).

Experimental

Synthesis of MWW-zeolite

Using hexamethyleneimine (HMI) as a template, we synthesized MWW-zeolites using a previously published protocol.[28–30]

Preparation of chiral salen

A chiral ligand was prepared from chiral amine and salicylaldehyde using a reported method and confirmed by ^{1}H, ^{13}C NMR & FTIR spectral data (shown in Fig. S1 to S3†).[31–33]

Zn(II) exchanged MWW-zeolite

A sample was prepared by mixing 5 grams of MWW-zeolite with 12 mmol of Zn(II) salt in 300 ml of deionized water with continuous stirring for 24 hours at 90 °C. As soon as the stirring period ended, the final product was isolated and washed numerous times with deionized water to remove any metal ions. Following this, the solid was dried at 120 °C for 15 hours.[34,35]

Synthesis of chiral Zn(II)–salen@MWW

A MWW-zeolite, in which Zn(II) ions were exchanged, was combined with an excess of chiral salen in a round flask. The ratio of metal to ligand was 0.33. The mixture was covered with an adequate amount of solvent and subjected to reflux for 24 hours under a flow of nitrogen gas. The unbound ligands were eliminated by extracting with acetone, and any Zn^{2+} ions that were not coordinated were removed *via* an ion-exchange process using a 0.1 M sodium chloride aqueous solution. Afterwards, the sample felt a complete washing process using deionized water, followed by air-drying for a duration of 60 minutes. This process led to the creation of a chiral Zn(II)–salen ligand securely encapsulated within the MWW-zeolite. Thus, the resulting product is referred to as the Zn(II)–salen@MWW catalyst (Scheme 1).[4,36–40]

Catalytic activity

In brief, a mixture of aniline, benzaldehyde, and acetophenone (each 1 mmol) was combined with 0.05 g Zn(II)–salen@MWW catalyst. The reaction mixture was subjected to ultrasonic waves using a bath sonicator. The reaction was allowed to continue for

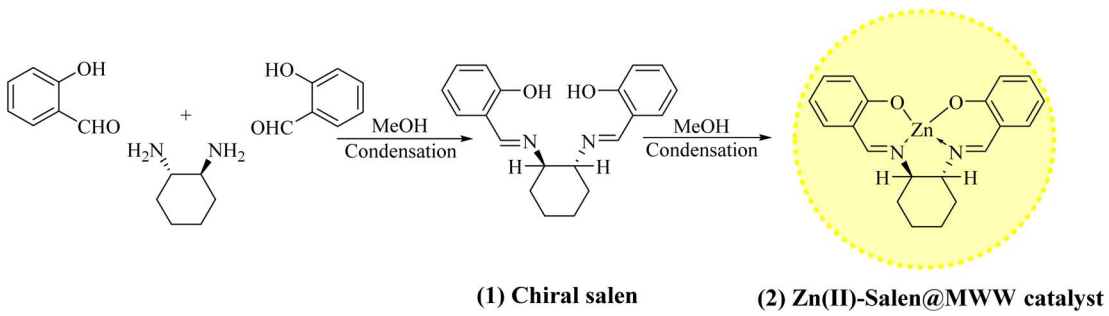

Scheme 1 A conceptual illustration of the preparation of chiral salen ligand (1) and Zn(II)–salen@MWW catalyst (2).

a duration of 120 minutes. Immediately after the accomplishment of the reaction, the solid catalyst was isolated from the crude solution by dissolving it in ethanol. After an exhaustive wash with ethanol, the catalyst was dried under vacuum so that it could be reused.[21,41,42]

Results and discussion

Powder X-ray diffraction (XRD) is a crucial method used to assess the level of crystallinity in powdered samples. Fig. 1 displays the XRD patterns of three samples: MWW-zeolite (a), Zn(II)-exchanged MWW-zeolite (b), and chiral Zn–salen@MWW catalyst (c). In all three samples, diffraction peaks are observed at 2θ values of 7.2°, 8.0°, 9.6°, 25°, and 26°, corresponding to the (100), (101), (102), (220), and (310) reflections, respectively. These peaks are distinctive characteristics of the MWW-zeolite. The results ensure that the crystalline arrangement of the MWW-zeolite remains intact after grafting.[43–46]

In Fig. 2 presents FE-SEM images of three samples: MWW-zeolite, Zn(II)-exchanged MWW-zeolite, and chiral Zn–salen@MWW. Fig. 2a shows the characteristic cube morphology of the primary crystals of MWW-zeolite. Fig. 2(b) and (c) demonstrate that the introduction of metal and scaffold produced minimal alterations in the surface morphology of the MWW-zeolite.[47–49]

Fig. S4(A) and (B)† exhibit N_2 adsorption–desorption isotherms and BJH pore size distributions for MWW-zeolite (a), Zn(II)-exchanged MWW-zeolite (b), and chiral Zn–salen@MWW (c). The hybrid materials demonstrate consistent pore size distributions within their mesoporous regions due to their type IV isotherm characteristics. These attributes validate the retention of the meticulously arranged mesoporous cage of MWW-zeolite within the synthesized materials. Table 1 presents a decrease in pore diameter, from 6.2 nm in pure MWW-zeolite to approximately 3.3 nm in Zn(II)-exchanged MWW-zeolite and 3.0 nm in chiral Zn(II)–salen@MWW. The BET surface area of the synthesized materials exhibits a gradual reduction, indicating the successful encapsulation of organic scaffolds onto the MWW-zeolite.[50]

Fig. S5† illustrates the FTIR spectral data of three samples: MWW-zeolite, Zn(II)-exchanged MWW-zeolite, and chiral Zn(II)–salen@MWW. In Fig. S5(a),† the FTIR spectra of MWW-zeolite reveals the presence of a prominent and wide band at 1015 cm^{-1}, indicating the occurrence of stretching vibration associated with aluminum silicate element. Conversely, the IR bands observed in the chiral Zn(II)-salen@MWW exhibit relatively weak intensities, which could be attributed to the lower concentrations of Zn(II)–salen present within the cage of MWW-zeolite. In the FTIR spectral data of the pure chiral salen ligand (Fig. S3†), a characteristic vibration of phenolic –OH is detected at 3450 cm^{-1}. However, in the chiral Zn(II)–salen@MWW, this vibration is notably absent, indicating the deprotonation of this group through coordination with the metal ion. The interaction of the nitrogen with the metal ion is assurance by the existence of a band at 1629 cm^{-1}. In spectra of chiral Zn(II)–salen complex, this band experiences a displacement towards the lower frequency range. The FTIR spectrum of chiral Zn(II)–salen complex encapsulated within the MWW-zeolite exhibits a prominent broad band around 3479 cm^{-1} these specific bands are indicative of –OH stretching, along with relatively less intense band in the around 804–816 cm^{-1} for rocking and 664–694 cm^{-1} wagging vibrations respectively, providing evidence for the presence of coordinated water molecules within the complex.[51]

Fig. S6† exhibits the results of the EDX analysis, confirming the existence of zinc, silica, aluminum, and oxygen elements in the composition of the chiral Zn(II)–salen@MWW.[52,53]

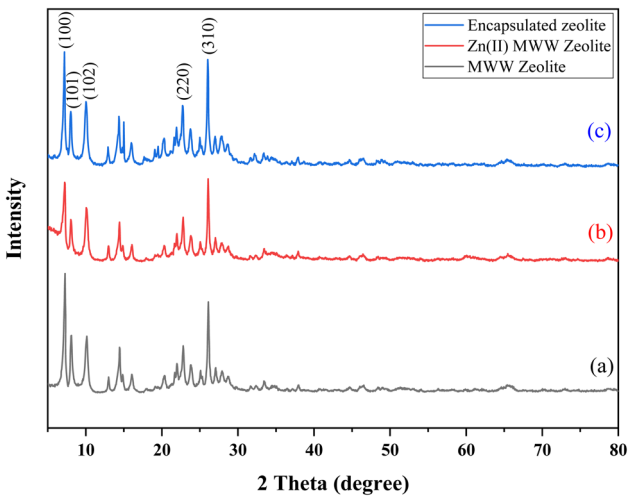

Fig. 1 XRD patterns of (a) MWW-zeolite (b) Zn(II)-exchanged MWW-zeolite (c) chiral Zn–salen@MWW catalyst.

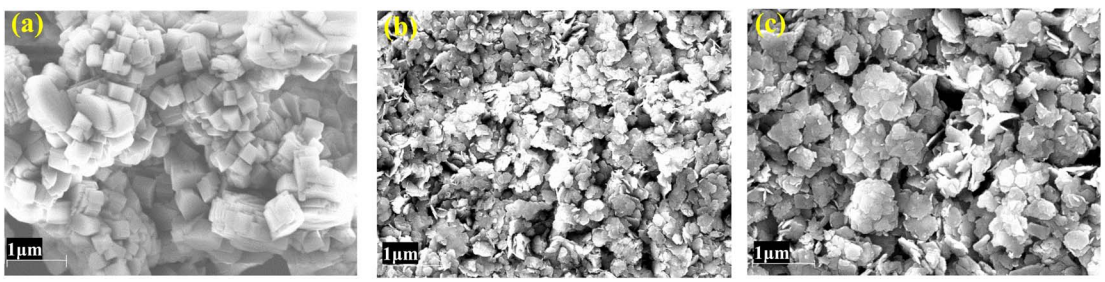

Fig. 2 FE-SEM results of (a) MWW-zeolite (b) Zn(II)-exchanged MWW-zeolite, (c) chiral Zn–salen@MWW.

Table 1 Porosity and texture features of catalyst and catalyst precursors

Sample	Surface area/m^2 g^{-1}	Pore volume/cm^3 g^{-1}	Average pore diameter/nm
MWW-zeolite	414.50	0.51	6.2
Zn(II)-exchanged MWW-zeolite	263.48	0.48	3.3
Chiral Zn(II)–salen@MWW	31.96	0.14	3.0

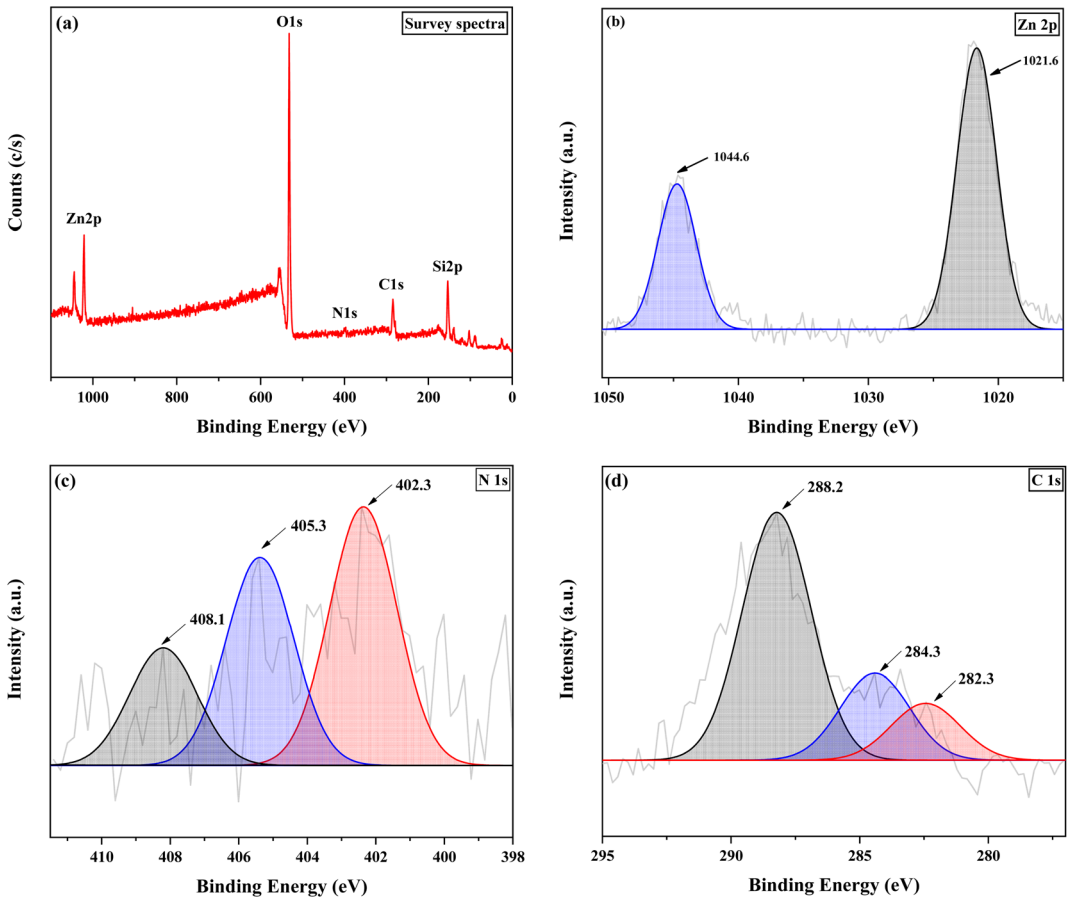

Fig. 3 XPS spectra of chiral Zn(II)–salen@MWW; (a) survey spectrum, (b) Zn 2p, (c) N 1s and (d) C 1s.

The data of the XPS analysis are shown in Fig. 3. This analysis was carried out to examine the surface elemental composition and elemental bonding of the chiral encapsulated Zn(II)–salen catalyst successfully prepared. The comprehensive XPS spectrum (Fig. 3a) demonstrates the existence of Zn, O, Si, C, and N elements. The XPS spectra of Zn 2p (Fig. 3b) exhibits peaks at 1021.6 eV for Zn 2p3/2 and 1044.6 eV for Zn 2p1/2, confirming the presence of Zn(II) within the sample. In the N 1s spectrum (Fig. 3c), three peaks at 402.3 eV (CN), 405.3 eV, and 408.1 eV are observed, indicating the interaction between zinc and nitrogen within the carbon moiety. Within the C 1s spectrum (Fig. 3d), three clearly distinguishable peaks are observed at 282.3 eV, 284.3 eV, and 288.2 eV, which analogous to chemical bonds C–C, C–O or C–N, and C=N, respectively.[54–59]

Chiral β-aminoketone derivatives synthesis

As a result of the successful fabrication and characterization of an chiral Zn(II)–salen@MWW, its catalytic property was assessed for use in one-pot Mannich reactions as shown in Scheme 2. An environmentally responsible, affordable, and economical reaction route is crucial when it comes to organic transformation reactions. There is one such effective route, *i.e.*, ultrasonic route, which has the advantages of being low energy-consuming, simple to react to, and quick to respond.

Initially, our focus was to establish an unpretentious method for synthesizing the target product. The use of a catalyst, howbeit, resulted in a higher yield. In ultrasonic-assisted reactions, ultrasonic radiation interacts with the organic substrate, creating transient cavities that are filled with liquid vapor or air.

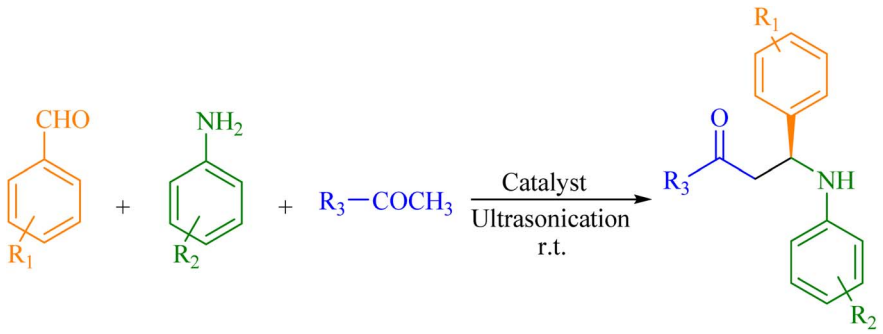

Scheme 2 Synthesis chiral β-aminoketone derivatives using chiral Zn(II)–salen@MWW.

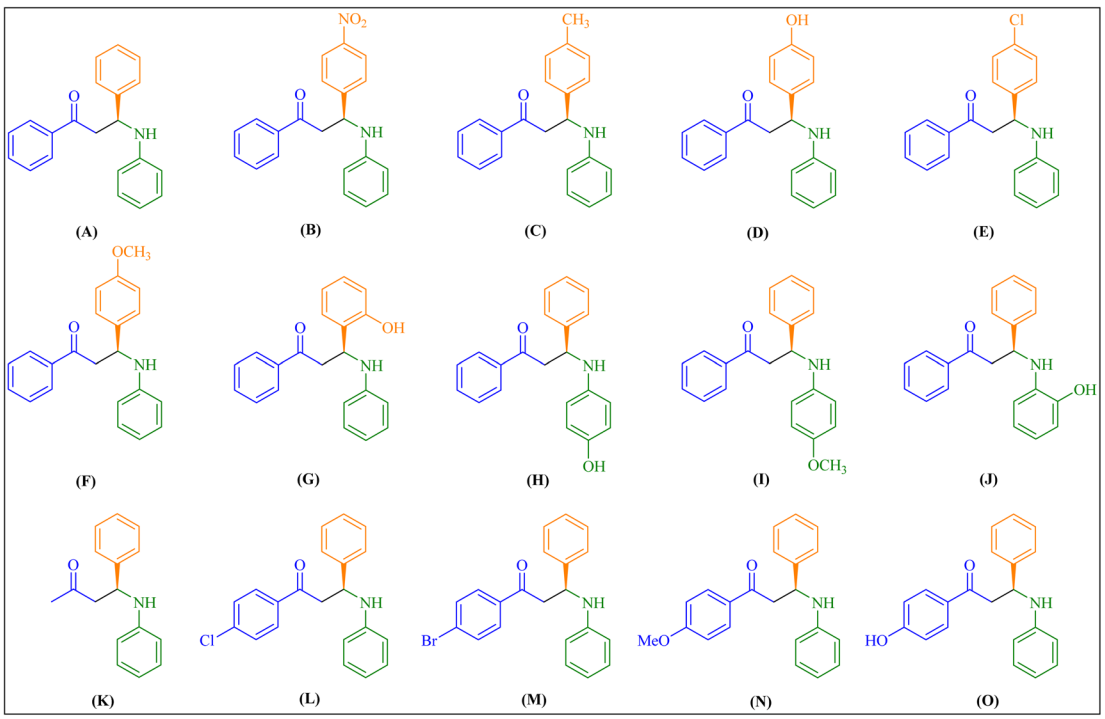

Fig. 4 Encapsulated chiral Zn(II)–salen complex catalyzes the synthesis of Mannich bases (A–O) derived from aryl ketone. Aldehyde/aniline/aryl ketone are in a 1 : 1 : 1 molar ratio.

These cavities collapse rapidly after a few ultrasound cycles, generating hot spots with high temperatures and pressures that help break chemical bonds and increase the yield of product in a less time. Through this process, mass flow mechanical energy is transformed into kinetic energy generated by arbitrary molecular translation and rotation. The method is advantageous because it eliminates the need for solvents, which can be associated with complex work-up procedures, safety concerns, high costs, and environmental problems.

To optimize the reaction conditions, we tested varied ratios of starting substrates and found that using 1 mmol of each substrate with a 1 : 1 : 1 ratio resulted in a high product yield. With optimized reaction conditions, we synthesized a different derivative of β-amino carbonyl compounds (Fig. 4) to evaluate our catalyst's efficiency and performance (Table 2). We also tested the upshot of substituents in aromatic aldehyde and aniline on product yield. In contrast to aldehydes with electron-donating substituents, those with electron-withdrawing groups produced a greater yield in fewer hours.

The products obtained were thoroughly analyzed chiral HPLC (shown in Fig. S7 to S25†) and confirmed by FTIR, ^{1}H & ^{13}C NMR spectral data (shown in Fig. S26 to S70†), and their data were compared with previously reported data. In addition to the synergistic effect among the individual components, the chiral Zn(II)–salen surface was able to adsorb significant amounts of reactant molecules, increasing its catalytic activity. Considering the above results, the presence of Brønsted and Lewis acidic sites, the synergistic effect amid the discrete components, and the larger surface area of the catalyst play crucial roles in its altogether catalytic performance. The activation of the reaction was further facilitated by ultrasonic wave through the preparation of β-amino carbonyl compounds.

Table 2 Chiral β-aminoketone derivatives synthesized through the one pot Mannich reaction with diverse substrates employing chiral Zn(II)–salen@MWW catalyst

Entry	Substrates (R_1, R_2 and R_3)	Product	Conversion (%)	ee[a] (%)
1	R_1 = –H; R_2 = –H; R_3 = –Ph	A	94	94.58
2	R_1 = 4-NO_2–; R_2 = –H; R_3 = –Ph	B	96	96.33
3	R_1 = 4-Me–; R_2 = –H; R_3 = –Ph	C	95	95.40
4	R_1 = 4-OH–; R_2 = –H; R_3 = –Ph	D	88	89.73
5	R_1= 4-Cl–; R_2 = –H; R_3 = –Ph	E	93	89.45
6	R_1 = 4-OMe–; R_2 = –H; R_3 = –Ph	F	89	88.00
7	R_1 = 2-OH–; R_2 = H–; R_3 = –Ph	G	81	84.07
8	R_1 = –H; R_2 = 4-OH–; R_3 = –Ph	H	87	91.82
9	R_1 = –H; R_2 = 4-OMe–; R_3 = –Ph	I	88	89.58
10	R_1 = –H; R_2 = 2-OH–; R_3 = –Ph	J	80	83.72
11	R_1 = –H; R_2 = –H; R_3 = $-CH_3$	K	95	94.35
12	R_1 = –H; R_2 = –H; R_3 = 4-Cl-Ph–	L	95	89.95
13	R_1 = –H; R_2 = –H; R_3 = 4-Br-Ph–	M	93	88.96
14	R_1 = –H; R_2 = –H; R_3 = 4-OMe-Ph–	N	86	87.67
15	R_1 = –H; R_2 = –H; R_3 = 4-OH-Ph–	O	84	86.98

[a] ee analyzed through chiral HPLC; reaction conditions: mole ratio of aldehydes, amine and ketone (1 : 1 : 1), and chiral Zn(II)–salen@MWW (0.05 g), ultrasonication, 120 min.

Table 3 Recyclability data of the chiral β-aminoketone derivatives synthesis

Entry	Product	Conversion (%)	ee[a] (%)
1	A1	94	94.58
2	A2	91	92.98
3	A3	89	87.83
4	A4	86	83.91
5	A5	85	82.44

[a] ee analyzed through chiral HPLC; reaction conditions: mole ratio of aldehydes, amine and ketone (1 : 1 : 1), and chiral Zn(II)–salen@MWW (0.05 g), ultrasonication, 120 min.

The catalyst's recyclability and stability are crucial for its effectiveness. To investigate this, we used the optimized conditions to assess the catalyst's reusability. As soon as the reaction was completed, the catalyst was recovered, washed with ethyl acetate to remove organic parts, and dried for 3 hours underneath vacuum at 80 °C. Despite reusing the chiral Zn(II)–salen@MWW catalyst five times, we observed only petite losses in catalytic activity. The fresh sample yielded 94% product yield and 94.58% ee as the catalytic run was being carried out, but these numbers somewhat fell to 85% and 82.44%, respectively, after the fifth run, as stated in Table 3 and their bar chart, which is displayed in Fig. S71.† In addition, the catalyst recovered after the 5th cycle has been characterized with FTIR and XRD, and it is compared with the fresh catalyst as shown in Fig. S72 & S73.†

Table 4 presents a comparison of chiral catalytic systems, both heterogeneous and homogeneous, utilized in chiral β-aminoketone synthesis. The results reveal that the present catalyst was compared to other previously reported catalysts and showed superior efficiency using a sustainable ultrasonic method, demonstrating higher activity within a short time frame.[13,60–66] Considering all the above results, a proposed mechanism can be made and is presented in Scheme 2. As a result of the acidic nature of the catalyst (Brønsted as well as Lewis) and the effective adhesion of reactant molecules to its surface, the reaction begins under ultrasonic irradiation. During the reaction, the carbonyl group of the aldehyde substrate is activated by protonation (predominantly by the acidic Brønsted sites of the active catalyst), while the Lewis acidic site activates aniline substrate. In the next step, the activated aldehyde is dehydrated by the nucleophilic aniline in order to form an iminium intermediate.

The asymmetric Mannich reaction of iminium intermediate with ketone had previously been reported to generate *in situ*

Table 4 A comparative study for the synthesis of the chiral β-aminoketone derivatives

Entry	Catalyst	Yield (%)	Time (hours)	Amount of catalyst (mol%)	Reference
1	$H_3PW_{12}O_{40}$	89	18	0.24	15
2	Sucrose char sulfonic acid	91	10	4	18
3	NH_2SO_3H	94	1.5	10	22
4	$Hf(OTf)_4$	89	6	5	53
5	NDPANI	94	7	4	55

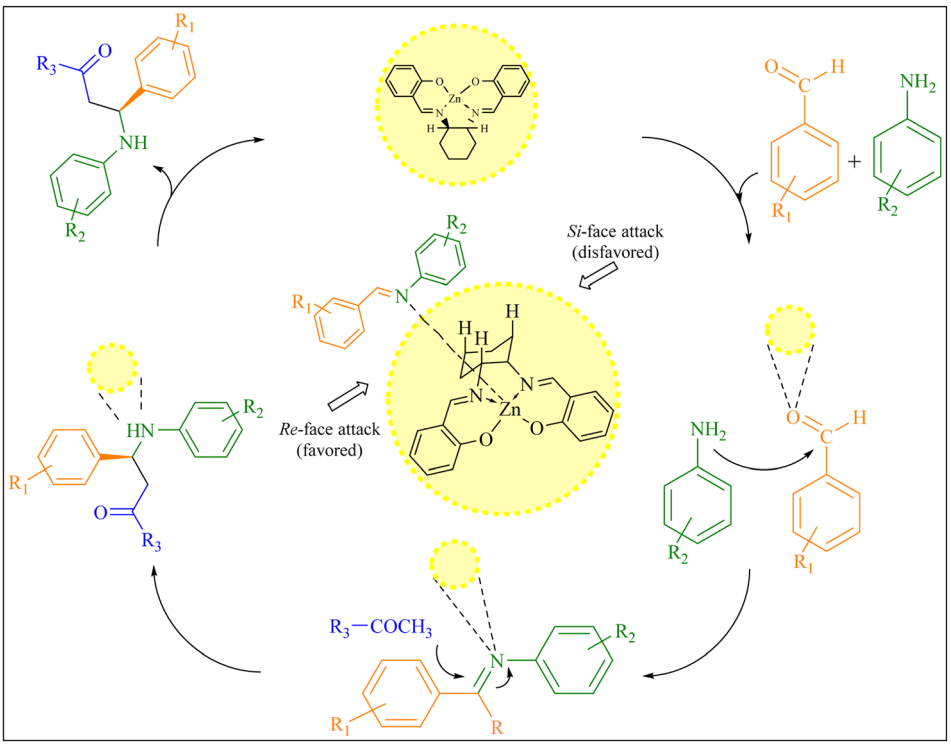

Fig. 5 A plausible reaction pathway for the chiral β-aminoketone derivatives synthesis and transition state models for the prediction of stereoselectivity.

metal complexes through axially chiral salen ligands (shown in Fig. 5). These transition states readily explain the observed *Re*-facial enantioselectivity is favored and the opposite selectivity (*Si*) is disfavored.[4]

Moreover, the desired product was efficiently produced by generating cavitation through ultrasonic irradiation. This process involved the formation and collapse of microbubbles, generating an enormous amount of thermal energy and district pressure that facilitated the fabrication of β-amino carbonyl compounds. The presence of acid groups on the catalyst, along with ultrasonic irradiation, favoured the dehydration process during the formation of the intermediate. Prior literature has referred to an analogous mechanism involving metal nanoparticles for the synthesis of β-aminocarbonyl compounds.

Conclusion

In this study, a highly persuasive, unprecedented and atypical encapsulated chiral Zn(II)–salen catalyst, Zn(II)–salen@MWW, was fabricated, characterized, and used to synthesize chiral β-amino carbonyls *via* a one-pot three-component using an ultrasonic irradiation. Related to other reported systems, the present catalyst demonstrated superior performance with a higher product yield 94% and (94.58 ee (%)) achieved in a shorter reaction time (120 min). Furthermore, the existence of acidic sites, a sky-scraping the area of surface, ultrasonic irradiation, and cooperative interaction among the discrete parts contribute to increased activity. Moreover, the catalyst exhibited remarkable reusability for up to five consecutive cycles, maintaining significant catalytic performance without substantial degradation. In summary, this study demonstrates that encapsulating chiral metal salen ligands on acidic zeolite surfaces can lead to highly effective, durable, and recyclable catalysts for various organic transformations.

Conflicts of interest

Conflicts of interest do not exist.

Acknowledgements

Mr Pratikkumar Lakhani would like to express his deepest gratitude to the Government of Gujarat, Gandhinagar, India, for awarding him the SHODH fellowship. It is our pleasure to acknowledge Mr Parimal Prabhat, I/C (PC&AL), Mr M. K. Tyagi, Scientific Assistant/F, and Mrs Pragyanditi Dash, Scientific Officer-E, Heavy Water Board Facilities, Vadodara, Gujarat, India, for recording NMR spectral data.

References

1 K. C. Nicolaou, *et al.*, A new method for the one-step synthesis of α,β-unsaturated carbonyl systems from saturated alcohols and carbonyl compounds, *J. Am. Chem. Soc.*, 2000, **122**, 7596–7597.
2 P. Lakhani and C. K. Modi, Shaping enantiochemistry: recent advances in enantioselective reactions *via*

heterogeneous chiral catalysis, *Mol. Catal.*, 2023, **548**, 113429.
3 V. P. Petrovic, V. P. Petrovic and Z. D. Petrovic, Acetophenone Mannich bases: study of ionic liquid catalysed synthesis and antioxidative potential of products, *R. Soc. Open Sci.*, 2018, **5**, 181232.
4 S. Shaw and J. D. White, Asymmetric Catalysis Using Chiral Salen-Metal Complexes: Recent Advances, *Chem. Rev.*, 2019, **119**, 9381–9426.
5 K. Alfonsi, *et al.*, Green chemistry tools to influence a medicinal chemistry and research chemistry based organisation, *Green Chem.*, 2008, **10**, 31–36.
6 R. K. Henderson, *et al.*, Green Chemistry Expanding GSK's solvent selection guide – embedding sustainability into solvent selection starting at medicinal chemistry, *Green Chem.*, 2011, **13**, 854–862.
7 D. J. C. Constable, C. Jimenez-Gonzalez and R. K. Henderson, Perspective on Solvent Use in the Pharmaceutical Industry, *Org. Process Res. Dev.*, 2007, **11**(1), 133–137.
8 S. Shamna, C. M. A. Afsina and M. Philip, Recent advances and prospects in the Zn-catalysed Mannich reaction, *RSC Adv.*, 2021, **11**, 9098.
9 P. Lakhani, *et al.*, DFT stimulation and experimental insights of chiral Cu(II)–salen scaffold within the pocket of MWW-zeolite and its catalytic study, *Phys. Chem. Chem. Phys.*, 2023, **25**, 14374–14386.
10 R. G. Da Silveira, *et al.*, Synthesis, Structure Determination and Catalytic Activity of a Novel Ruthenium(II) [RuCl(dppb)(44bipy)(4-pic)]PF6 Complex, *J. Braz. Chem. Soc.*, 2021, **32**, 1802–1812.
11 B. H. Rotstein, S. Zaretsky, V. Rai and A. K. Yudin, Small heterocycles in multicomponent reactions, *Chem. Rev.*, 2014, **114**, 8323–8359.
12 J. M. M. Verkade, L. J. C. Van Hemert, J. L. M. Quaedflieg and F. P. J. T. Rutjes, Organocatalysed asymmetric Mannich reactions, *Chem. Soc. Rev.*, 2008, **37**, 29–41.
13 A. Kumar, M. K. Gupta and M. Kumar, Green Chemistry catalysed multicomponent synthesis of 3-amino alkylated indoles *via* a Mannich-type reaction under solvent-free conditions, *Green Chem.*, 2012, **14**, 290–295.
14 A. Kumar, M. K. Gupta and M. Kumar, An efficient non-ionic surfactant catalyzed multicomponent synthesis of novel benzylamino coumarin derivative *via* Mannich type reaction in aqueous media, *Tetrahedron Lett.*, 2011, **52**, 4521–4525.
15 N. Azizi, L. Torkiyan and M. R. Saidi, Highly Efficient One-Pot Three-Component Mannich Reaction in Water Catalyzed by Heteropoly Acids, *Org. Lett.*, 2006, **8**, 10.
16 N. Azizi, R. Baghi, E. Batebi and S. M. Bolourtchian, Catalytic stereoselective Mannich reaction under solvent-free conditions, *C. R. Chim.*, 2012, **15**, 278–282.
17 J. Iwanejko, E. Wojaczyńska and T. K. Olszewski, Green chemistry and catalysis in Mannich reaction, *Curr. Opin. Green Sustainable Chem.*, 2018, **10**, 27–34.
18 Q. Xu, Z. Yang, D. Yin and J. Wang, One-pot three-component Mannich reaction catalyzed by sucrose char sulfonic acid, *Front. Chem. Eng. China*, 2009, **3**(2), 201–205.
19 H. Yonghai, S. Wei, S. Xie, C. Wang and X. Zhengfeng, Three-Component Mannich Reaction Catalyzed by MCM-41 Immobilized H3PW12O40 (PW) in Water, *Chin. J. Org. Chem.*, 2014, **34**, 1212–1217.
20 S. A. Ozturkcan, K. Turhan and Z. Turgut, Ultrasound-assisted rapid synthesis of β-aminoketones with direct-type catalytic Mannich reaction using bismuth(III)triflate in aqueous media at room temperature, *Chem. Pap.*, 2012, **66**(1), 137–147.
21 L. S. K. Achary, P. S. Nayak, B. Barik, A. Kumar and P. Dash, Ultrasonic-assisted green synthesis of β-amino carbonyl compounds by copper oxide nanoparticles decorated phosphate functionalized graphene oxide *via* Mannich reaction, *Catal. Today*, 2020, **348**, 137–147.
22 H. Zeng, H. Li and H. Shao, Ultrasonics sonochemistry one-pot three-component Mannich-type reactions using sulfamic acid catalyst under ultrasound irradiation, *Ultrason. Sonochem.*, 2009, **16**, 758–762.
23 P. Lakhani and C. K. Modi, Spick-and-span protocol for designing of silica-supported enantioselective organocatalyst for the asymmetric aldol reaction, *Mol. Catal.*, 2022, **525**, 112359.
24 P. Lakhani and C. K. Modi, Asymmetric Hydrogenation using Covalently Immobilized Ru-BINOL-AP@MSNs Catalyst, *New J. Chem.*, 2023, **47**, 8767–8775.
25 W. Chu, *et al.*, Effect of Binder Type on MWW-Based Catalysts for the Liquid-Phase Alkylation Reaction of Benzene with Ethylene, *Ind. Eng. Chem. Res.*, 2022, **61**, 2693–2700.
26 S. Jin, *et al.*, A facile organosilane-based strategy for direct synthesis of thin MWW-type titanosilicate with high catalytic oxidation performance, *Catal. Sci. Technol.*, 2018, **8**, 6076–6083.
27 Y. Zhou, *et al.*, Enhanced Surface Activity of MWW Zeolite Nanosheets Prepared *via* a One-Step Synthesis, *J. Am. Chem. Soc.*, 2020, **142**, 8211–8222.
28 A. Ahmad, S. R. Naqvi, M. Rafique, H. Nasir and A. Sarosh, Synthesis, characterization and catalytic testing of MCM-22 derived catalysts for n-hexane cracking, *Sci. Rep.*, 2020, **10**, 1–11.
29 A. Schwanke and S. Pergher, Lamellar MWW-type zeolites: toward elegant nanoporous materials, *Appl. Sci.*, 2018, **8**, 1636.
30 J. Krishna Reddy, K. Mantri, S. Lad, J. Das, G. Raman and R. v. Jasra, Synthesis of Ce-MCM-22 and its enhanced catalytic performance for the removal of olefins from aromatic stream, *J. Porous Mater.*, 2020, **27**, 1649–1658.
31 A. A. Shiryaev, *et al.*, A chiral (1R,2R)-N,N′-bis-(salicylidene)-1,2-diphenyl-1,2-ethanediamine Schiff base dye: synthesis, crystal structure, Hirshfeld surface analysis, computational study, photophysical properties and *in silico* antifungal activity, *J. Iran. Chem. Soc.*, 2021, **18**, 2897–2911.

32 C. Baleizão and H. Garcia, Chiral salen complexes: an overview to recoverable and reusable homogeneous and heterogenous catalysts, *Chem. Rev.*, 2006, **106**, 3987–4043.
33 G. Yuan, H. Jiang, L. Zhang, Y. Liu and Y. Cui, Metallosalen-based crystalline porous materials: synthesis and property, *Coord. Chem. Rev.*, 2019, **378**, 483–499.
34 K. Motokura, S. Ding, K. Usui and Y. Kong, Enhanced Catalysis Based on the Surface Environment of the Silica-Supported Metal Complex, *ACS Catal.*, 2021, **11**, 11985–12018.
35 C. K. Modi, P. M. Trivedi, S. K. Gupta and P. K. Jha, Transition metal complexes enslaved in the supercages of zeolite-Y: DFT investigation and catalytic significance, *J. Inclusion Phenom. Macrocyclic Chem.*, 2012, **74**, 117–127.
36 F. Uhrmacher, S. M. Elbert, F. Rominger and M. Mastalerz, Synthesis of Large [2+3] Salicylimine Cages with Embedded Metal-Salphen Units, *Eur. J. Inorg. Chem.*, 2022, **2022**, 1–9.
37 H. Kargar, *et al.*, Synthesis, spectral characterization, and theoretical investigation of Ni(II) and Pd(II) complexes incorporating symmetrical tetradentate Schiff base ligand: Suzuki-Miyaura cross-coupling reaction using PdLSym, *J. Iran. Chem. Soc.*, 2022, **19**, 3981–3992.
38 S. Yimthachote, P. Chumsaeng and K. Phomphrai, Complexity of imine and amine Schiff-base tin(II) complexes: drastic differences of amino and pyridyl side arms, *Dalton Trans.*, 2022, **51**, 509–517.
39 Y. C. Yuan, M. Mellah, E. Schulz and O. R. P. David, Making Chiral Salen Complexes Work with Organocatalysts, *Chem. Rev.*, 2022, **122**, 8841–8883.
40 G. Gbery, A. Zsigmond and K. J. Balkus, Enantioselective epoxidations catalyzed by zeolite MCM-22 encapsulated Jacobsen's catalyst, *Catal. Lett.*, 2001, **74**, 77–80.
41 B. List, The Direct Catalytic Asymmetric Three-Component Mannich Reaction, *J. Am. Chem. Soc.*, 2000, **122**(38), 9336–9337.
42 L. S. Longo and M. V. Craveiro, Deep Eutectic Solvents as Unconventional Media for Multicomponent Reactions, *J. Braz. Chem. Soc.*, 2018, **29**, 1999–2025.
43 A. Moezzi, M. B. Cortie and A. M. Mcdonagh, Zinc hydroxide sulphate and its transformation to crystalline zinc oxide, *Dalton Trans.*, 2013, **42**, 14432–14437.
44 A. Kazemi, M. Salavati-niasari and A. Khansari, Solvent-less synthesis of zinc oxide nanostructures from Zn (salen) as precursor and their optical properties Particuology Solvent-less synthesis of zinc oxide nanostructures from Zn (salen) as precursor and their optical properties, *Particuology*, 2012, **10**, 759–764.
45 S. Cao, *et al.*, "Desert Rose" MCM-22 microsphere: synthesis, formation mechanism and alkylation performance, *Microporous Mesoporous Mater.*, 2021, **315**, 110910.
46 R. Thakkar and R. Bandyopadhyay, Preparation, characterization, and post-synthetic modification of layered MCM-22 zeolite precursor, *J. Chem. Sci.*, 2017, **129**, 1671–1676.
47 M. Juneau, *et al.*, Characterization of Metal-zeolite Composite Catalysts: Determining the Environment of the Active Phase, *ChemCatChem*, 2020, **12**, 1826–1852.
48 J. Chen, *et al.*, Catalytic performances of cu/mcm-22 zeolites with different cu loadings in nh3-scr, *Nanomaterials*, 2020, **10**, 1–20.
49 S. Srilai, *et al.*, Synthesis of zeolite A from bentonite *via* hydrothermal method: the case of different base solution, *AIP Conf. Proc.*, 2020, **2279**, 060006.
50 Y. Yang, Y. Zhang, S. Hao and Q. Kan, Tethering of Cu(II), Co(II) and Fe(III) tetrahydro-salen and salen complexes onto amino-functionalized SBA-15: effects of salen ligand hydrogenation on catalytic performances for aerobic epoxidation of styrene, *Chem. Eng. J.*, 2011, **171**, 1356–1366.
51 C. K. Modi and P. M. Trivedi, Zeolite-Y based nanohybrid materials: synthesis, characterization and catalytic aspects, *Microporous Mesoporous Mater.*, 2012, **155**, 227–232.
52 C. S. Carriço, *et al.*, MWW-type catalysts for gas phase glycerol dehydration to acrolein, *J. Catal.*, 2016, **334**, 34–41.
53 A. H. Kianfar, *et al.*, Experimental and theoretical structural determination, spectroscopy and electrochemistry of cobalt (III) Schiff base complexes: immobilization of complexes onto Montmorillonite-K10 nanoclay, *J. Iran. Chem. Soc.*, 2018, **15**, 369–380.
54 J. Sun, H. Fan, B. Nan and S. Ai, Fe3O4@LDH@Ag/Ag3PO4 submicrosphere as a magnetically separable visible-light, *Photocatalyst*, 2014, **130**, 84–90.
55 A. Khalid, *et al.*, Enhanced Optical and Antibacterial Activity of Hydrothermally Synthesized Cobalt-Doped Zinc Oxide Cylindrical Microcrystals, *Materials*, 2021, **14**(12), 3223.
56 M. Claros, M. Setka, Y. P. Jimenez and S. Vallejos, AACVD Synthesis and Characterization of Iron and Copper Oxides Modified ZnO Structured Films, *Nanomaterials*, 2020, **10**(3), 471.
57 A. A. Abd El Khalk, M. A. Betiha, A. S. Mansour, M. G. Abd El Wahed and A. M. Al-Sabagh, High Degradation of Methylene Blue Using a New Nanocomposite Based on Zeolitic Imidazolate Framework-8, *ACS Omega*, 2021, **6**, 26210–26220.
58 R. S. Vithalani, *et al.*, Synthesis of less acidic VO–salen complex grafted onto graphene oxide *via* functionalization of surface carboxyl groups for the selective oxidation of norbornene, *Graphene Technol.*, 2020, **5**, 83–101.
59 S. Chao, *et al.*, Nitrogen-doped Carbon Derived from ZIF-8 as a High-performance Metal-free Catalyst for Acetylene Hydrochlorination, *Sci. Rep.*, 2017, **7**, 1–7.
60 M. Gil-ord, C. Aubry, C. Niño, A. Maestro and J. M. Andrés, Squaramide-Catalyzed Asymmetric Mannich Reaction between 1,3-Dicarbonyl Compounds and Pyrazolinone Ketimines: A Pathway to Enantioenriched 4-Pyrazolyl- and 4-Isoxazolyl-4-aminopyrazolone Derivatives, *Molecules*, 2022, **27**(20), 6983.
61 S. Han, J. Wei, X. Peng, R. Liu and S. Gong, Hf(OTf)4 as a Highly Potent Catalyst for the Synthesis of Mannich Bases under Solvent-Free Conditions, *Molecules*, 2020, **25**(2), 388.
62 M. Kiani, H. Anaraki-Ardakani, N. Hasanzadeh and A. Rayatzadeh, Fe3O4@saponin/Cd: a novel magnetic nano-catalyst for the synthesis of β-aminoketone derivatives, *J. Iran. Chem. Soc.*, 2020, **17**, 2243–2256.

63 S. Behera and B. N. Patra, One-pot synthesis of β-amino carbonyl compounds under solvent free condition by using alum doped nanopolyaniline catalyst, *Polymer*, 2021, **228**, 123851.

64 S. Saikia, P. Gogoi, A. K. Dutta, P. Sarma and R. Borah, Chemical Design of multifaceted acidic 1, 3-disulfoimidazolium chlorometallate ionic systems as heterogeneous catalysts for the preparation of β -amino carbonyl compounds, *J. Mol. Catal. A: Chem.*, 2016, **416**, 63–72.

65 N. Azizi and M. Edrisi, Deep eutectic solvent immobilized on SBA-15 as a novel separable catalyst for one-pot three-component Mannich reaction, *Microporous Mesoporous Mater.*, 2016, **240**, 130–136.

66 P. Ganwir and G. U. Chaturbhuj, Aluminized Polyborate: A New and Eco-friendly Catalyst for One-pot Multicomponent Synthesis of Reaction, *Org. Prep. Proced. Int.*, 2022, **54**, 338–345.